Electronic Supplementary Material (ESI) for RSC Advances.

Supporting Information

Interface Modification Strategy Based on Hybrid Cathode Buffer Layer for Promoting the Performance of Polymer Solar Cells

Feng Ye,[abc] Zhaobin Chen,[b] Xiaoli Zhao,[a] Zidong Li[abc] and Xiaoniu Yang*[a]

[a] State Key Laboratory of Polymer Physics and Chemistry, Changchun Institute of Applied Chemistry, Chinese Academy of Sciences, 5625 Renmin Street, Changchun 130022, P.R. China.

[b] Polymer Composites Engineering Laboratory, Changchun Institute of Applied Chemistry, Chinese Academy of Sciences, 5625 Renmin Street, Changchun 130022, P.R. China.

[c] University of Chinese Academy of Sciences, 19 Yuquan Road Shijingshan District, Beijing 100049, P.R. China

*Corresponding author. E-mail address: xnyang@ciac.jl.cn; Fax: +86-0431-85262028; Tel.:+86-0431-85262206. (Xiaoniu Yang)

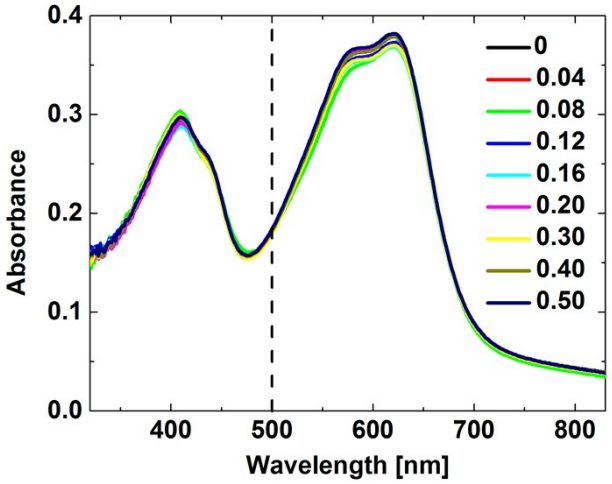

Fig. S1 Absorbance of PBDT-TFQ films deposited on FPDA:PFN blend films with weight ratio ranging from 0 to 0.50.

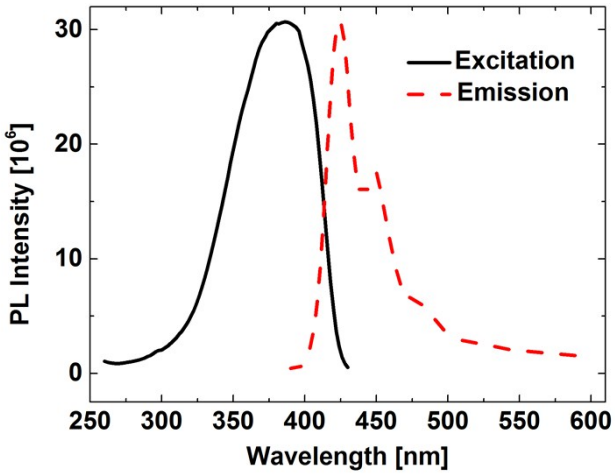

Fig. S2 Fluorescence excitation spectrum (solid line, emission offset fixed at 440nm) and emission spectrum (dash line, excited at 380nm) of PFN film.

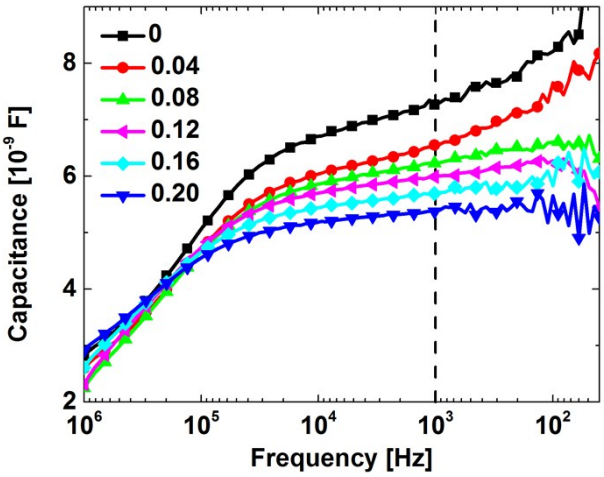

Fig. S3 *C-f* plots of the devices structured as Ag/MoO_3/PBDT-TFQ/HCBL/ITO with various FPDA:PFN ratio.

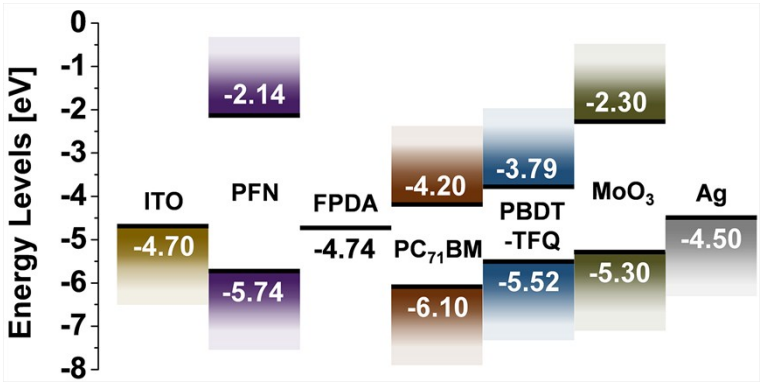

Fig. S4 Energy level diagrams for all components in the inverted photovoltaic devices with configuration of Ag/MoO_3/PBDT-TFQ:$PC_{71}BM$/HCBL/ITO/glass.

It is noted that the Lewis base FPDA plays its role of regulating carrier extraction in terms of interface state modification, but not as the host material for energy band alignment, which indicates the necessity to reach a certain range of FPDA:PFN ratio for the achievement of a desired effect. With the FPDA:PFN ratio less than 0.40, the hole-blocking ability turn out to be positively correlated with the FPDA content. However, when the FPDA:PFN ratio is further increased to a degree as 0.50, the hole-blocking effect sharply subsides into the form of low-resistance short circuit (shown in Fig. S4). This may be attributed to a substituted conductive path established by the excessive FPDA and energy band alignment effect of the host material is subsided with the barrier breakdown.

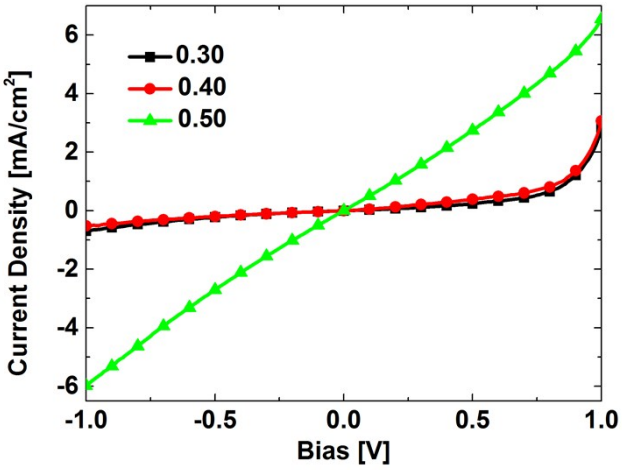

Fig. S5 *J-V* characteristics of the devices structured as Ag/MoO_3/PBDT-TFQ/HCBL/ITO with FPDA:PFN ratio of 0.30, 0.40 and 0.50 respectively.

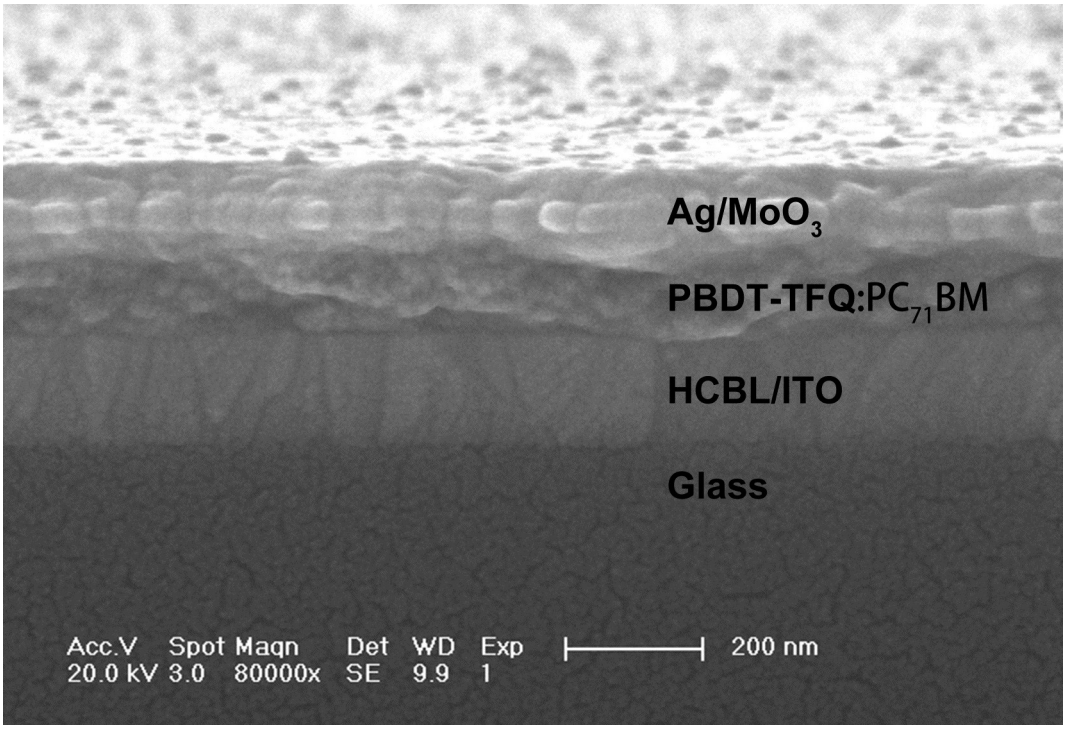

Fig. S6 Cross-section SEM image of the inverted photovoltaic device with configuration of Ag/MoO_3/PBDT-TFQ:$PC_{71}BM$/HCBL/ITO/glass.

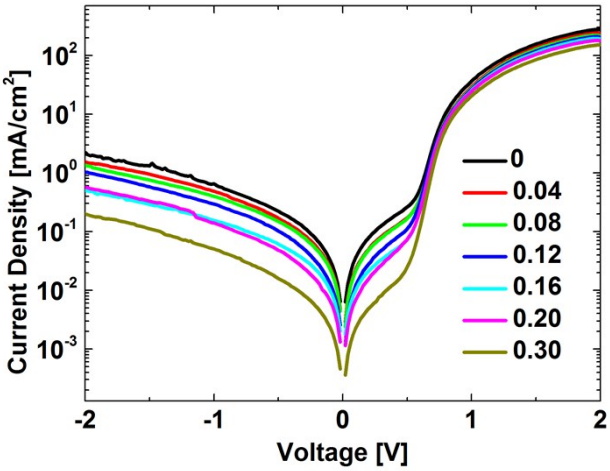

Fig. S7 *J*-*V* characteristics of the devices with HCBL of series FPDA:PFN ratios under dark condition.

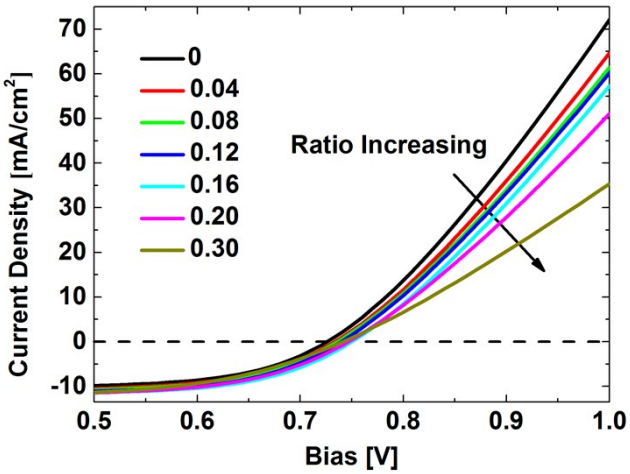

Fig. S8 Device *J*-*V* response in the bias range of carrier injection.

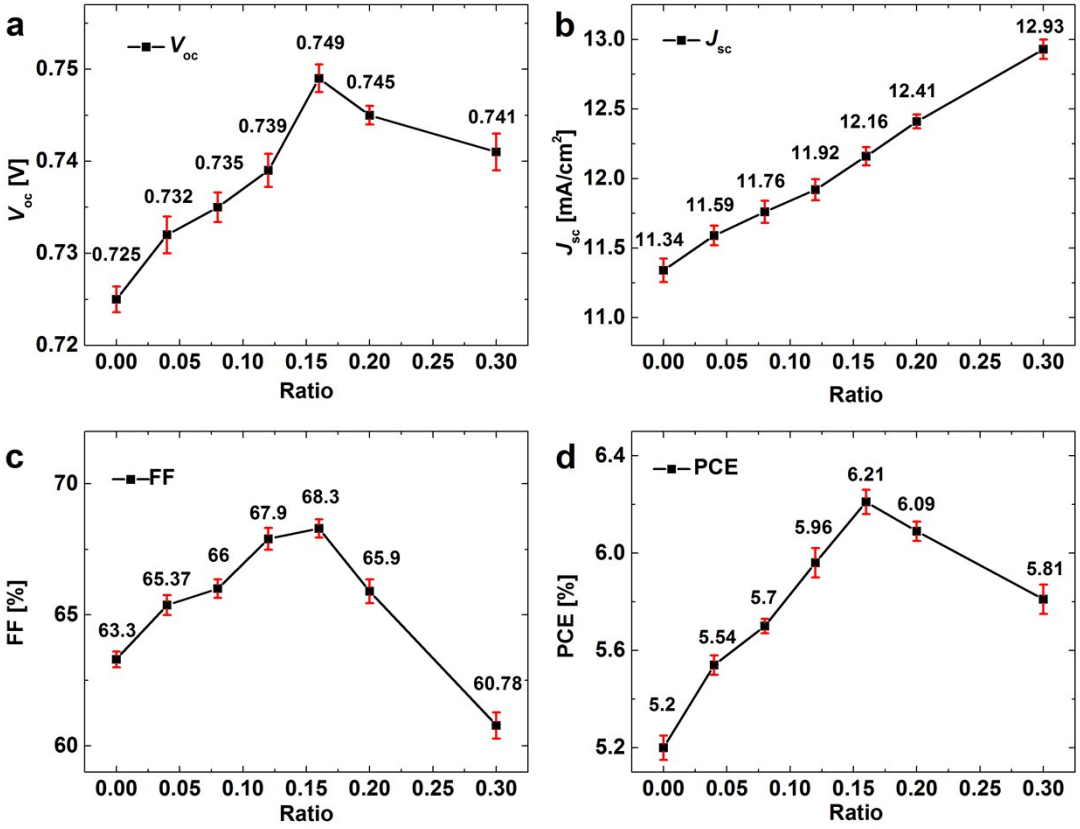

Fig. S9 Statistical analysis of (a) V_{oc}, (b) J_{sc}, (c) FF and (d) PCE for 8 devices with the average values labelled correspondingly.

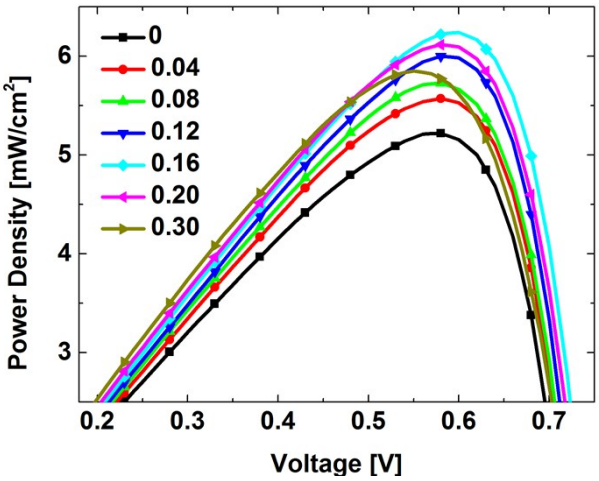

Fig. S10 Device *P*-*V* curves based on HCBL of series FPDA:PFN ratio.

Table S1 Fit results of the equivalent circuit for the Nyquist plots of devices with HCBL of different

Bias [V]	FPDA:PFN=0			FPDA:PFN=0.08			FPDA:PFN=0.20		
	C_p [nF]	R_s [Ω]	R_p [10^3Ω]	C_p [nF]	R_s [Ω]	R_p [10^3Ω]	C_p [nF]	R_s [Ω]	R_p [10^3Ω]
0	7.27	17.4	7.40	6.23	23.9	11.40	5.37	30.6	75.00
0.2	11.28	18.7	6.00	8.50	32.9	10.20	6.51	34.8	52.80
0.4	17.29	26.7	4.62	14.37	34.5	9.00	10.65	22.5	41.80
0.6	19.66	22.6	3.40	17.21	31.8	6.90	13.64	33.9	21.00
0.8	22.27	23.8	0.80	19.62	16.8	3.40	15.83	20.6	2.70
1.0	N/A	N/A	N/A	26.17	22.3	0.37	22.63	21.9	0.37

FPDA:PFN ratio.

Table S2 Fit results of the Mott-Schottky analysis of the *C-V* plots.

FPDA:PFN	0	0.04	0.08	0.12	0.16	0.20
N_A [10^{16} cm^{-3}]	10.07	9.32	9.41	8.27	8.14	7.23
V_b [V]	0.33	0.38	0.42	0.43	0.46	0.50